EasyChair Preprint

№ 7298

Simulation of Combustion in an Internal Combustion Engine by the Converge Code

Nardjes Bengherbia and Mohamed Roudane

January 5, 2022

Simulation of Combustion in an Internal Combustion Engine by the Converge Code

Nardjes Bengherbia[a], Mohamed Roudane [b].

[a,b] Fundamental and applied physics laboratory FUNDAPL
Mechanical Enginneering Departement Faculty of Technologie
University of Blida 1
BP270 Blida 09000 Algeria
nardjesbengherbia@gmail.com

ABSTRACT

Lately, petrol engines have undergone a remarkable evolution thanks to their outstanding performance despite the emission of polluting gases. The reheating of the Earth's atmosphere, depletion of natural resources, and the increasing Toughening of the anti-pollution standards have pushed scientists to study seriously the physical phenomena and chemical phenomena of burning in order to decrease the emission of polluting gases through the fuel reformulation while maintaining engine performance. We begin this study with generalities on internal combustion engines. Then we will make an overview of the fuels, after that we quote the mathematical formulations as well the chemical and physical models. In the end, we present the concentrations of different polluting species: NOx, Soot Particles, unburned hydrocarbon HC and carbon monoxide CO calculated numerically using the CONVERGE code for the two fuels: iso-pentane ($C5H12$) and heptan ($C7H16$) engine with direct injection by introducing the chemical kinetics reactions of NO and the total reaction of oxidation of the fuel and equilibrium reactions contributing in the formation of the pollutants

1. INTRODUCTION

The movement of a mass is always linked to kinetic energy which results from a potential which can be of thermal origin, such is the case of the role of an internal combustion engine which transforms the combustion of the fuel into a movement of the crankshaft. Depending on the fuel ignition and combustion mode, there are two main classes of engines[1]: internal combustion engines current constraints, both ecological and economic, are forcing automakers to carry out research related to turbulent combustion and its applications. Therefore it is necessary to understand the predominant physical and chemical processes within a combustion chamber not only to allow the improvement of current systems but also the development of new technologies. In this context, the use of digital tools makes it possible to reduce costs and study times. It is very easy to digitally modify the geometry or the conditions of use (pressure, temperature, etc.). The investigations carried out with CFD codes (in English Computational Fluid Dynamics) for example CONVERGE, Fluent, and CFX… [2] then make it possible to test a large number of solutions to retain only the most relevant for experimental tests. In the context of modeling turbulent combustion, the use of a computer code such as KIVA or CONVERGE represents a good approach to understanding and predicting the phenomena that appear inside the cylinder of a combustion engine. internal. Within the framework of this work we used the code of CONVERGE V1.3. The internal combustion engine is a driving machine which is used to convert the energy stored in a fuel (calorific value) into thermal energy (heat; enthalpy, calorific energy)[3]; then into mechanical energy (mechanical work; torque). in internal combustion engines; the production of thermal energy takes place in a closed volume (chamber of combustion; engine cylinder) confined by the cylinder head; valves closed; piston head and liner. the expansion of the gases produced by the combustion of the fuel activates active organs (pistio-connecting rod - Crank) which recover this energy to convert it into useful work (Arbe engine). Combustion engines can be classified into different categories. The two most important are based on the combustion process (positive ignition and compression ignition). And the work cycle (2 stroke vs 4 stroke). Further classification may be based on the air supply (naturally aspirated or supercharged), the injection (indirect or direct injection), and the cooling system (air or water).

2. GOVERNING EQUATION AND NUMERICAL APPROACH

The mathematical modeling of a turbulent flow with or without a chemical reaction is conventionally carried out using the resolution of nonlinear and coupled partial differential equations. These equations express the principles of conservation of mass, momentum, and chemical species in an elementary volume of fluid.

2.1. The continuity equation of the chemical species m

The determination of the mass fraction for each species, m, is done by the solution of the transport equation of the th species, which has the following form

$$\frac{\partial \rho_m}{\partial t} + \nabla.(\rho_m u) = \nabla.[\rho D \nabla (\frac{\rho_m}{\rho})] + \rho_m^c + \rho^s \delta_{m1} \quad (1)$$

Where ρ_m the density of the species, ρ is the total density, and u is the velocity of the fluid with ρc and ρs the source terms due to the chemistry and the spray respectively.
We assume that all species have equal diffusivities, given by D = $\frac{\mu}{\rho SC}$

μ is the dynamic viscosity and Sc is the Schmidt number (the Schmidt number compares the effects of Viscosity and diffusion of the fluid), $S_c = \frac{v}{D}$.

2.2. The total mass conservation equation

By summing equation (1) for all species we obtain the equation for the total density of the fluid

$$\frac{\partial \rho}{\partial t} + \nabla (\rho.u) = \dot{\rho}^s \quad (2)$$

So the mass is conserved in chemical reactions

2.3. The momentum equation

The equation for conservation of momentum of the mixture is given by

$$\frac{\partial \rho u}{\partial t} + \nabla (\rho.u.u) = -\frac{1}{\alpha^2}\nabla p - A_0 \nabla(\frac{2}{3}\rho k) + \nabla\sigma + F^S + \rho g \quad (3)$$

Is used in conjunction with the PGS (Pressure Gradient Scaling) method. α Where p is the pressure of the fluid. The quantity In equation (3) the quantity A_0 is zero for laminar flows, and unity if one of the turbulence models are used. The tensor of the viscous stresses is of Newtonian form

$$\sigma = \mu [\nabla u (\nabla u)^T] \lambda \nabla.u \quad (4)$$

Will be defined in what follows. The exponent T indicates the transpose of a matrix and I represent the unit matrix. Fs is the rate of momentum per unit volume gain due to vaporization. The force of inertia g is considered constantλ and μ the two viscosity coefficients.

2.4. The energy equation:

The internal energy equation I is, exclusive to chemical energy

$$\frac{\partial \rho I}{\partial t} + \nabla. (\rho u I) = -p \nabla.u + (1-A_0) \sigma : \nabla.J + A_0 \rho\varepsilon + \dot{Q}^C + \dot{Q}^S \quad (5)$$

The thermal flux vector J is the sum of the contributions due to thermal conduction and the diffusion of enthalpy

$$J = -KVT - \rho D \sum m\, h_m \nabla (\frac{\rho_m}{\rho}) \quad (6)$$

Where T is the temperature of the fluid and the species-specific enthalpy m, K is the thermal conductivity. K Is calculated from the Prandtl number and the specific heat at constant pressure.

3. NUMERICAL MODELING

We have simulated the Caterpillar 3401 engine using the CONVERGE code with different fuel injection times, the version of the code used exploits the characteristic time combustion (CTC) model for the

C7H16 and wise for the C5H12. To validate the numerical results we refer to the setting of the pressure curve while considering the engine at medium load 1600 rpm.

3.1. Engine specification :

Table 1. Description of the geometric characteristics of the engine studied.

Settings	**Specifications**
Motor type	Caterpillar 3401
Cylinder diameter	13.716 cm
The race	16.51 cm
Connecting rod length	26.3 cm
Length between cylinder head and piston in PMH	0.4221 cm
Compression ratio	15.1

Table 2. Description of the characteristics of the injection system of the engine studied.

Fuel injection system	
Fuels	$C7H16$
Mode of injection	Profile
Injection system	Common Rail
Diameter of the injection hole	$2.6.10^{-4}$
Duration of injection	21 degree
Start of injection	-9 deg A PMH
The temperature of the fuel injected	341 K
Numbers des Bec	6

3.2. Physicochemical property of fuel used:

For the fuel chosen, the parameters necessary for the simulation are shown in the table below

Table 3. Physico-chemical property of fuel used [Annex].

Fuel	C5H12 (pentane)	C7H16 (heptane)	C8H18 (octane)
Densité (g/ml)	0.618	0.68	0.691

3.3. Choice of simulation models

Table 4. choice of models.

	Process	**Model**
1	Combustion	SAGE – CTC
2	Turbulence	RNG k-ε
3	Ignition delay	Shell
4	Atomization	KH-RT
5	Heat transfer	Wall law

3.4. Initial conditions :

As for the initial conditions, we introduced the pressure "pres_init", the chamber temperature "temp_init", the kinetic energy "tke_init", and the dissipation rate "eps_init". The data is shown in the table 5.

Table 5. Initial conditions.

Régime = 1600 tr/min	
pres_init [Pa]	1.9700e+05
temp_init [K]	355
tke_init [m^2/s^2]	62.02710
eps_init [m^2/s^3]	17183.40

3.5. Limit conditions:

The boundary conditions are given by the cylinder head temperatures Tcu, the cylinder Tcy and the piston base Tp. The data is shown in table 6.

Table 6. Limit conditions.

Régime = 1600 tr/min	
Tcu [K]	523.0
Tcy [K]	433.0
Tp [K]	553.0

4. RESULTS

4.1. Medium pressure:

Figure (1) shows the pressure as a function of the crankshaft angle. The maximum average pressure is reached at TDC. The air is compressed up to 8 MPA before TDC but in the combustion phase it increases up to 10.8 MPA for the C7H16 and 12 MPA for the C5H12. We noticed that the pressure peak in the cylinder for the case of C5H12 is more important than C7H16. This is due to the ignition delay .On the other hand we noticed that the peak pressure in the cylinder in the case of C5h12 and C7H16 present a slight difference of about 5% . Therefore a greater combustion in the case of C5H12 which results in a greater pressure peak in the combustion chamber.

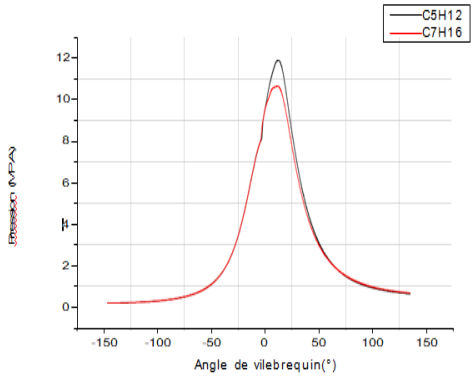

Fig1. the pressure as a function of the crankshaft angle

4.2. Average cycle temperature:

Figure (2) represents the temperature as a function of the crankshaft angle The temperature remains constant during the admission (temperature of the fresh gases), then increases slowly during the compression phase. Then there is a small decrease in the temperature which is due to the elementary influence of the fuel injected at a cold temperature on the general temperature of the combustion chamber. after that a significant jump is imported into the curves and this latter means that the flame has taken a large volume in the combustion chamber . Then the temperature drops during the expansion and exhaust phase the maximum average temperature reached is of the order of 1800k and 1600k respectively for the C5H12 and the C7H16.

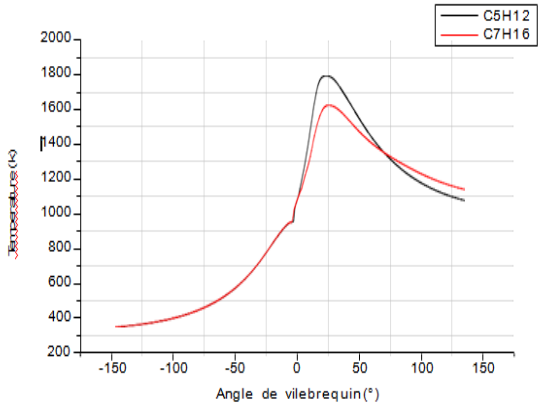

Fig 2.temperature as a function of crankshaft angle

4.3. Formation of polluting gases:

➢ Nitrogen oxide

Figure (3) shows the evolution of NOx as a function of the crankshaft angle for the different fuels. The rise in the concentration of NOx manifests it self in a rapid manner just after the start of combustion. the walls of the cylinder. This drop in temperature dampens the chemistry of the NOx and their concentration remains relatively constant. We notice that C5H12 has high NOx emissions compared to C7H16. This is probably due to the high temperature in the combustion chamber and the difficulty of local mixing despite a higher oxygen level in the C5H12 fuel.

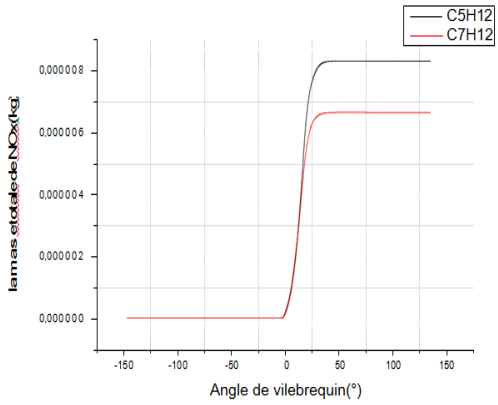

Fig3. the total mass of NOx as a function of the crankshaft angle

➢ Carbon monoxide :

Figure (4) represents the mass of Co as a function of the crankshaft angle The evolution of carbon monoxide CO as a function of the crankshaft angle for the fuels tested is illustrated in the figure. Incomplete combustion naturally generates CO which increases rapidly during the combustion phase of premixed by default of oxygen at the local level. However during the diffusion phase the CO oxidizes to form CO2 and this because of the excess air in the chamber. We notice that the CO increases at the start of combustion up to 16 * 10-5kg and 20 * 10-5kg respectively for C5H12 and C7H16 which is due to the richness of the fuel mixture (excess of O2) and their decrease is explained by the lean mixture.

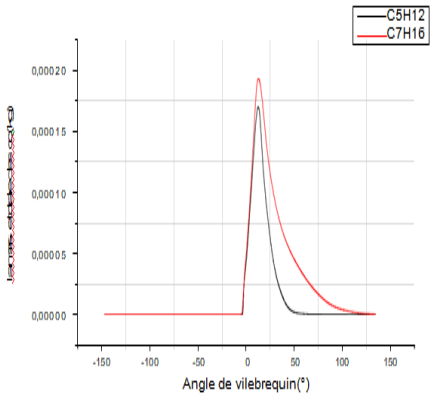

Fig4: the total mass of CO as a function of the crankshaft angle

➢ Hydrocarbons

Figure (5) shows the evolution of unburnt hydrocarbons as a function of the crankshaft angle. Note that the emission of HC in the exhaust gas are mainly due to the zones of sub-mixing or superposition and to the quenching of the walls . The HC emission increases during the period of premelenger combustion reaching their peak at the end of this stage . It decreases to reach the minimum.

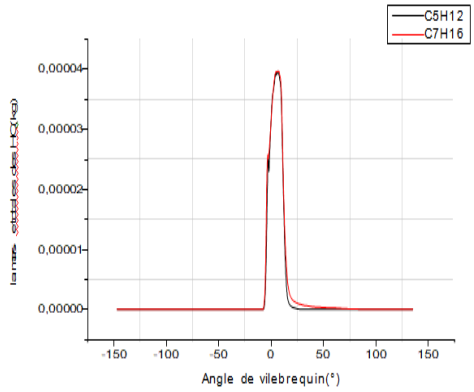

Fig5 :prediction of HC as a function of the crankshaft angle

4.4. Contours plot

➢ Pollutant gas storyteller:

Figure (6) shows the contour of NOx and soot at different angles of the crankshaft (5 °, 10 °, 40 ° and 70 ° after TDC) for the C7h16 and C5h12 fuel. We notice The figure represents the temperature fields for the C7H16 fuel tested at different crankshaft angles (5 °, 10 °, 19 ° and 40 ° after TDC) we notice that the concentration of NOx and the mass of soot increases because of the high temperature in the combustion chamber for the angles 5 ° and 10 °, and for the angles 40 ° and 70 ° the temperatures of the burnt gases decrease due to their expansion and because of heat transfers through the walls of the cylinder. This drop in temperature dampens the chemistry of the NOx.

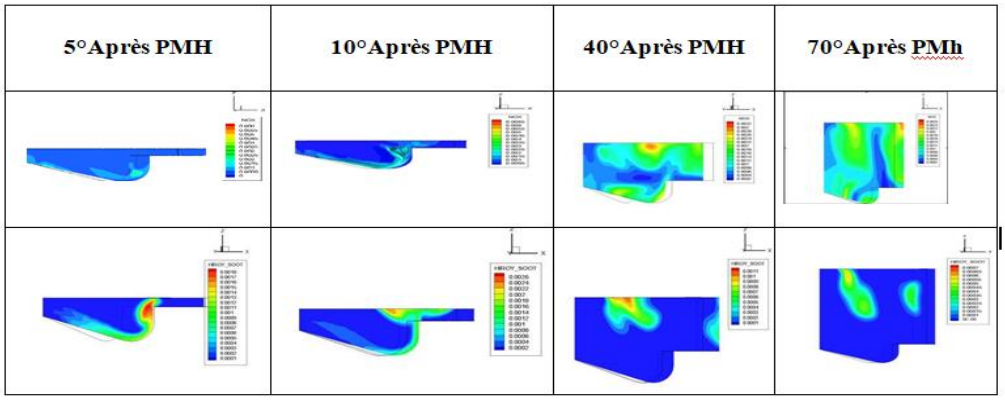

Fig 6. Contour of the mass of NOx and soot of fuel C7H16 and C5H12

➢ Evolution of the jet (the mass of injected fuel):

Figure (7) shows the contours of the fuel injected at different crankshaft angles (5 °, 10 °, 40 ° and 70 ° after TDC) for C7h16 and C5h12 fuels tested. From the analysis of the contours, it is clear that the evolution of the jet for fuels at 5 °and 10 ° after TDC is to be taken the same because of the properties of the latter (viscosity, density).

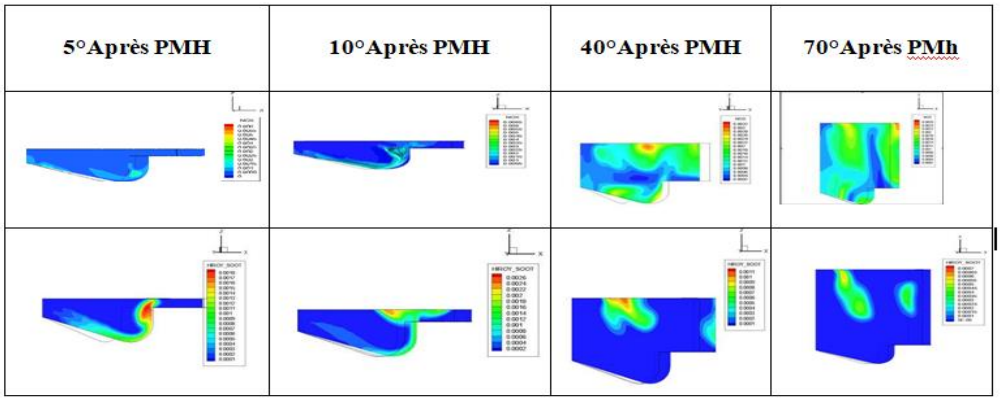

Fig. 7. Contours of the mass of fuel C7H16 and C5H12

5. CONCLUSION

The CTC combustion model is well suited for biofuels. The various results found make it possible to analyze, on an intra-cycle scale, the mechanical and energy performance (rate of heat released and temperature of the gases), as well as the emissions of various pollutants (NOx, HC, CO). Illustrations of dynamic and scalar contours (temperature, NOx) were presented and discussed.
The results obtained show that the increase in the NOx concentration manifests itself rapidly after the start of combustion. HC emissions increase sharply during the pre-mixed combustion period and decrease to minimum at the end of the combustion phase. CO oxidizes to form CO2 due to excess air in the chamber, which dissociates into CO.

REFERENCES

[1] K.J. Richards, P.K. Senecal, and E. Pomraning, «A Three-Dimensional Computational Fluid Dynamics Program for Transient or Steady State Flows with Complex Geometries », CONVERGE (Version 1.3), Convergent Science, Inc, Middleton,WI. (2008).

[2] C. Correa**,** « Combustion Simulations in Diesel Engines using Reduced Reaction Mechanism », thèse de doctorat, University of heidelberg 2000.

[3] D. Jung and D. N. Assanis, « Multi-zone Diesel spray combustion model for cycle simulation studies of engine performance and emissions », SAE paper 2001-01-1246, 2001.